9th Asia-Pacific Conference on Wind Engineering
Auckland, New Zealand
3-7 December 2017

On Appropriate Value of Flight Parameter in Numerically Simulating Trajectories of Wind-borne Rectangular Rod

Y. Eguchi[1], T. Murakami[1], S. Sugimoto[1] and Y. Hattori[1]

[1]Nuclear Risk Research Center
Central Research Institute of Electric Power Industry, Abiko 1646, Abiko-shi, Chiba-ken, 270-1194 JAPAN

Abstract

Two kinds of flight parameter coefficient sets for a rectangular rod are examined in terms of appropriateness in numerically simulating flight trajectories. Rod motions observed in a wind tunnel experiment of Texas Tech University were selected as the reference to be compared with the numerical flight trajectories. The results indicate that a set of the flight parameter coefficients used by Simiu and Scanlan (1996) is absolutely conservative, while that by Maruyama *et al.* (2014) is practically conservative to represent the upper bound of the effective drag force during flight with tumbling. Discussion based on the cross-flow theory, previous experimental data and the averaging technique for static drag force with random orientation suggests that the conservative features of both the coefficient sets will be reasonably applicable to a rod with the other aspect ratios.

Introduction

Strong wind in hurricanes/typhoons and tornadoes can induce air-borne debris or missiles. To protect human life, key assets and others of our concern, we need to evaluate how significant the missile impact is and to provide protection against it, if necessary. In particular, we have to pay our attention to slender objects such as a rod, because wind-borne rods may pierce outer envelopes of buildings and facilities, leading to potential threat to the insides. To understand such risk induced by the wind-borne missiles, computational evaluation of missile motion has often been employed. Physical models to simulate the missile trajectories can be classified into three as reviewed by Twisdale and Vickery [12]; 3-D (degree-of-freedom) model, random orientation 6-D model and full 6-D model. The 3-D model takes only drag force into account in the translational equations, while the random orientation 6-D model and the full 6-D model additionally consider lift force and side forces [8, 9]. In the 3-D model, a user has to select appropriate value of flight parameter, which is proportional to the product of effective drag and effective projection area during dynamic motion, so that a computed trajectory can reasonably represent an actual flight path.

The objective of this study is to examine the appropriateness of two sets of flight parameter coefficients proposed by Simiu and Scanlan [10] and Maruyama *et al.* [6] with particular focus on a rectangular rod. The experimental results obtained in a wind tunnel of Texas Tech University by Lin *et al.* [3, 4, 5] are used for comparison with numerical flight trajectories obtained with the two sets of flight parameter coefficients. In the following section, we explain the theoretical background including the basic equations of the 3-D model, non-dimensional quantities, flight parameter coefficients and the Lin's experiment. After explaining the numerical scheme and conditions employed in this study, we show the comparison between the numerical and experimental results. Then, insight into the aspect ratio effect on the effective drag coefficient during dynamic motion of a rod in flight are developed through discussions, and conclusions are drawn in final.

Theoretical Background

Let us consider a wind-borne rectangular rod, whose edge lengths are L, d and b, where $L>>d\geqq b$, as shown in Figure 1. The basic equations of the 3-D model can be written as follows with the missile velocity, (u, v, w) and the wind velocity, (U_x, U_y, U_z).

$$\frac{du}{dt}=\frac{\rho[C_DA]}{2m}(U_x-u)\sqrt{(U_x-u)^2+(U_y-v)^2+(U_z-w)^2} \quad (1a)$$

$$\frac{dv}{dt}=\frac{\rho[C_DA]}{2m}(U_y-v)\sqrt{(U_x-u)^2+(U_y-v)^2+(U_z-w)^2} \quad (1b)$$

$$\frac{dw}{dt}=\frac{\rho[C_DA]}{2m}(U_z-w)\sqrt{(U_x-u)^2+(U_y-v)^2+(U_z-w)^2}-g \quad (1c)$$

In the above equations, the following notations are used;

m: mass of rod, t: time, ρ: air density, $[C_DA]/m$: flight parameter, g: gravitational acceleration

Equations (1) can be non-dimensionalized as follows with a representative speed, U.

$$\frac{d\underline{u}}{d\underline{t}}=\frac{[C_DA]}{Ld}K(\underline{U}_x-\underline{u})\sqrt{(\underline{U}_x-\underline{u})^2+(\underline{U}_y-\underline{v})^2+(\underline{U}_z-\underline{w})^2} \quad (2a)$$

$$\frac{d\underline{v}}{d\underline{t}}=\frac{[C_DA]}{Ld}K(\underline{U}_y-\underline{v})\sqrt{(\underline{U}_x-\underline{u})^2+(\underline{U}_y-\underline{v})^2+(\underline{U}_z-\underline{w})^2} \quad (2b)$$

$$\frac{d\underline{w}}{d\underline{t}}=\frac{[C_DA]}{Ld}K(\underline{U}_z-\underline{w})\sqrt{(\underline{U}_x-\underline{u})^2+(\underline{U}_y-\underline{v})^2+(\underline{U}_z-\underline{w})^2}-1 \quad (2c)$$

where non-dimensional velocities, ($\underline{u}$, $\underline{v}$, $\underline{w}$) , ($\underline{U}_x$, $\underline{U}_y$, $\underline{U}_z$), and non-dimensional time, $\underline{t}$, are related with the dimensional ones such that; $\underline{u}=u/U$, $\underline{U}_x=U_x/U$ and $\underline{t}=gt/U$. Non-dimensional quantity, K, is called Tachikawa number and is defined as below.

$$K=\frac{\rho U^2Ld}{2mg} \quad (3)$$

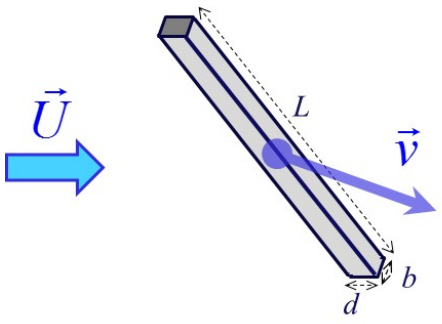

Figure 1. Missile flying at velocity $\vec{v}$ =(u,v,w) under influence of a wind field $\vec{U}$ =(U_x,U_y,U_z).

The Tachikawa number, K, can be definitely estimated *a priori* with measurable quantities. On the other hand, $[C_DA]$ is not easily known in general, because $[C_DA]$ may be influenced possibly by dynamic effect, turbulence [2], roundness of edges [1] and aspect ratio, d/b [7]. In the previous literatures [6, 10], the following form was used for engineering estimate of $[C_DA]$.

$$[C_DA] = c(C_{Ld}Ld + C_{Lb}Lb + C_{db}db) \quad (4)$$

However, the coefficients, c, C_{Ld}, C_{Lb} and C_{db}, in the above formula in [6] are different from those in [10] as seen in Table 1.

Reference	c	C_{Ld}	C_{Lb}	C_{db}
Simiu and Scanlan [10]	1/2	2.0	2.0	2.0
Maruyama *et al.* [6]	1/3	1.2	1.2	2.0

Table 1. Coefficients used to estimate a flight parameter [6, 10].

Lin's Wind Tunnel Experiment [3, 4, 5]

Lin [3] conducted wind tunnel experiments at Texas Tech University to observe flight motions of 4 kinds of rods (Table 2) under straight wind condition. Initially, the rods were hold static with the main axis orientation parallel to the stream (perfectly parallel if angle of attack is zero), or perpendicular to the stream. The initial angle of attack was varied at 15° and 45° other than 0°. The K values ranged from 3.8 to 27.7. The flight trajectories captured with a video camera were processed and compiled in terms of $K\underline{x}$ versus $K\underline{t}$, where non-dimensional horizontal displacement, $\underline{x}$, is defined as gx/U^2 with horizontal dimensional displacement, x. Lin [3] and the related literatures [4, 5] indicate that $K\underline{x}$ can be expressed in the following fitting curves.

For rods released perpendicular to the wind,

$$K\underline{x} \approx 0.40(K\underline{t})^2 - 0.16(K\underline{t})^3 + 0.036(K\underline{t})^4 - 0.0032(K\underline{t})^5 \quad (5).$$

For rods released parallel to the wind,

$$K\underline{x} \approx 0.40(K\underline{t})^2 - 0.29(K\underline{t})^3 + 0.088(K\underline{t})^4 - 0.0082(K\underline{t})^5 \quad (6).$$

No.	L	d	b	m
Rod1	381.0mm	12.7mm	6.4mm	17.9g
Rod2				6.0g
Rod3	330.2mm			5.5g
Rod4				9.8g

Table 2. Specification of rods used in the wind tunnel experiment [3].

Numerical Scheme and Conditions

Numerical solutions can be obtained with Equation (1a) to (1c) by an explicit time integration such that,

$$\mathbf{V}(t+\Delta t) = \mathbf{V}(t) + \frac{\partial \mathbf{V}(t)}{\partial t}\Delta t \quad (7)$$

$$\mathbf{X}(t+\Delta t) = \mathbf{X}(t) + \mathbf{V}(t)\Delta t + \frac{\partial \mathbf{V}(t)}{\partial t}\frac{\Delta t^2}{2} \quad (8)$$

where $\mathbf{V}(t)$ and $\mathbf{X}(t)$ are the velocity and displacement vectors of a missile at t=t, respectively, and Δt is the time increment. The time derivative of $\mathbf{V}(t)$ can be computed *via* Equation (1a) to (1c) with a prescribed wind velocity (U_x, U_y, U_z)=$(U,0,0)$ and known values of $\mathbf{X}(t)$ and $\mathbf{V}(t)$. Then, $\mathbf{X}(t+\Delta t)$ and $\mathbf{V}(t+\Delta t)$ can be easily obtained using Equations (7) and (8). In this study, Δt, g and ρ are respectively set at 0.001s, 9.80665m/s^2 and 1.226kg/m^3, while the wind speed U is set at 15.0m/s and 23.45m/s so that the corresponding K values take 3.8 and 27.7, respectively, which are the lower and upper bounds of the Lin's experimental conditions described in the references [3, 4, 5]. We note that the wind speed described in [3] are 12, 16 and 25 m/s, which are a little different from the wind speed corresponding to the K values for unknown reason. The numerical cases computed in this study are tabulated in Table 3 for the coefficients, c, C_{Ld}, C_{Lb} and C_{db}, of Simiu and Scanlan [10] and Table 4 for those of Maruyama *et al.* [6].

Comparison with the Lin's Experimental Results

The numerical results of horizontal displacement at each time step (x, t) were converted into non-dimensional form ($K\underline{x}$, $K\underline{t}$) and compared with the experimental fitting curves obtained by Lin [3, 4, 5] as shown in Figure 2 (a) and (b).

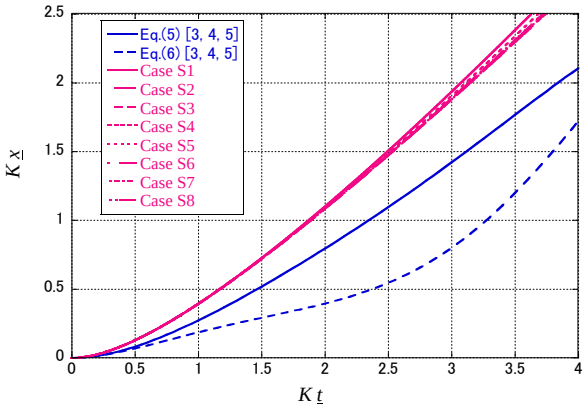

(a) Numerical results with coefficients used by Simiu and Scanlan [10]

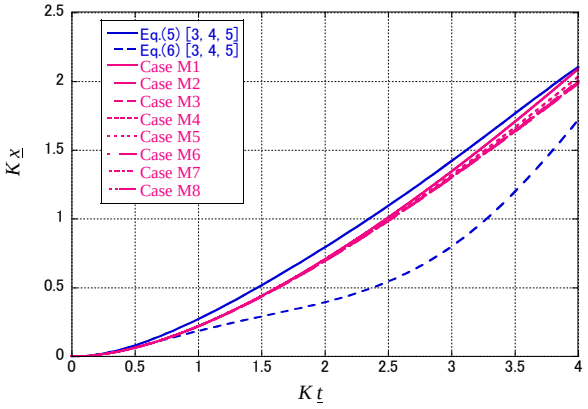

(b) Numerical results with coefficients used by Maruyama *et al.* [6]

Figure 2. Comparison of the Lin's experimental results [3, 4, 5] and numerical results: (a)upper: Case S1-S8, (b)above: Case M1-M8.

Case no.	Rod type	U (m/s)	$[C_DA]/m$ (m^2/kg)	K (-)
S1	Rod1	15.0	0.411	3.80
S2	Rod2		1.226	11.3
S3	Rod3		1.161	10.7
S4	Rod4		0.652	6.02
S5	Rod1	23.45	0.411	9.29
S6	Rod2		1.226	27.7
S7	Rod3		1.161	26.2
S8	Rod4		0.652	14.7

Table 3. Numerical cases with coefficients used by Simiu & Scanlan [10].

Case no.	Rod type	U (m/s)	$[C_DA]/m$ (m^2/kg)	K (-)
M1	Rod1	15.0	0.166	3.80
M2	Rod2		0.494	11.3
M3	Rod3		0.469	10.7
M4	Rod4		0.263	6.02
M5	Rod1	23.45	0.166	9.29
M6	Rod2		0.494	27.7
M7	Rod3		0.469	26.2
M8	Rod4		0.263	14.7

Table 4. Numerical cases with coefficients used by Maruyama *et al.* [6].

Discussion

The results of Figure 2(a) and (b) indicate that the flight parameter coefficients suggested by Simiu and Scanlan [10] is very conservative, and that those by Maruyama *et al.* [6] enables to represent the upper bound of the effective drag force during translational motion with tumbling.

As previously mentioned, $[C_DA]$ could be influenced possibly by dynamic effect, turbulence [2], roundness of edges [1] and aspect ratio, d/b [7]. In particular, Nakaguchi *et al.* [7] observed interesting dependency of the static drag coefficient on the aspect ratio as shown in Figure 3. In the following, we shall discuss the effect of the aspect ratio on $[C_DA]$. Our discussion is based on the cross-flow theory and the static drag force averaged for random orientation in the same way as that for a circular cylinder employed by Twisdale *et al.* [11, 12]. Assuming that the cross-flow principle holds true, the product of drag coefficient and projected area of a rectangular rod in arbitrary orientation, (α,β), and yaw angle γ, $[C_DA]_{\alpha,\beta,\gamma}$, can be expressed as below [12].

$$[C_DA]_{\alpha,\beta,\gamma} = bdC_{bd}\left|\cos^3\alpha\right| + LdC_{Ld}\left|\cos^3\gamma\right|\sin^3\alpha + LbC_{Lb}\left|\sin^3\gamma\right|\sin^3\alpha \quad (9)$$

In the above, the angles of α, β and γ are those defined in Figure 4, while C_{bd}, C_{Ld} and C_{Lb} are drag coefficients when each rod face is right to the incident angle. Assuming that the angles of α, β and γ are completely random, we can compute the expected value of $[C_DA]_{\alpha,\beta,\gamma}$, *i.e.* $[C_DA]_C$, using the following integration.

$$[C_DA]_C = \int_0^{\pi}\int_0^{2\pi}\int_0^{2\pi}[C_DA]_{\alpha,\beta,\gamma}\, f(\alpha,\beta,\gamma)\,d\gamma\,d\beta\,d\alpha \quad (10)$$

where $f(\alpha,\beta,\gamma)$ is the joint probability density function, defined as below.

$$f(\alpha,\beta,\gamma) = \frac{\sin\alpha}{8\pi^2} \quad (11)$$

Substituting Equations (9) and (11) into Equation (10) leads to the following relation.

$$[C_DA]_C = \frac{1}{4}\left(C_{Ld}Ld + C_{Lb}Lb + C_{bd}bd\right) \quad (12)$$

We can see the above is identical to Equation (4) if one sets c at 1/4 there. Since L is usually much larger than d and b, the last term in Equation (4) is negligible and the effective drag coefficient, $[C_DA]/Ld$, can be calculated as follows.

$$\frac{[C_DA]}{Ld} \approx c\left(C_{Ld} + C_{Lb}\frac{b}{d}\right) \quad (13)$$

Figure 5 shows the effective drag coefficient, $[C_DA]/Ld$, in variation with the aspect ratio, d/b. The values of C_{Ld} and C_{Lb} for $[C_DA]_C$ are calculated using the fitting curve for the Nakaguchi's experimental results (solid and dashed lines in Figure 3). It is seen in Figure 5 that the effective drag coefficient computed with the coefficients of Maruyama *et al.* [6] is rather close to the semi-theoretical value of $[C_DA]_C/Ld$ over the wide range of the aspect ratio, d/b. Considering the fact that corner roundness at rod edges tends to significantly reduce the drag coefficient of a rectangular rod in general [1], it is expected that the gap between the two curves will be narrowed in practical situations. On the other hand, the effective drag coefficient computed with the coefficients of Simiu and Scanlan [10] is about two times larger than the others over the whole range of the aspect ratio, d/b. These suggest that the features observed in the comparative study of the Lin's experiment and numerical results for d/b=1.98 will be generally applicable to a rod with different aspect ratio.

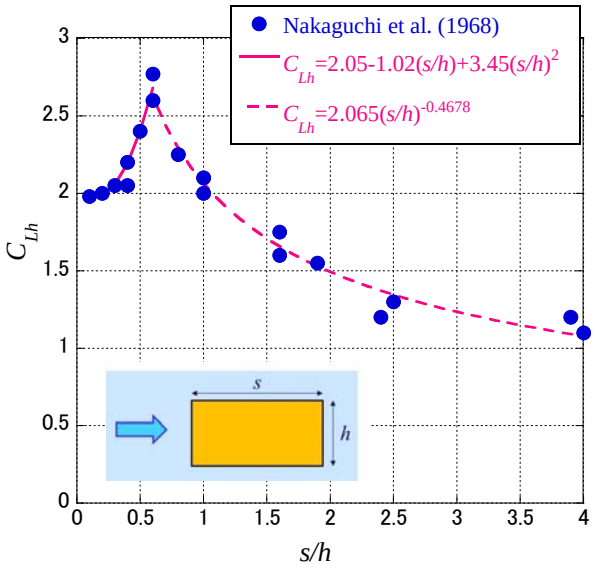

Figure 3. Drag coefficient for a long rectangular rod in variation with aspect ratio s/h [7] with the fitting curve (solid and dashed lines).

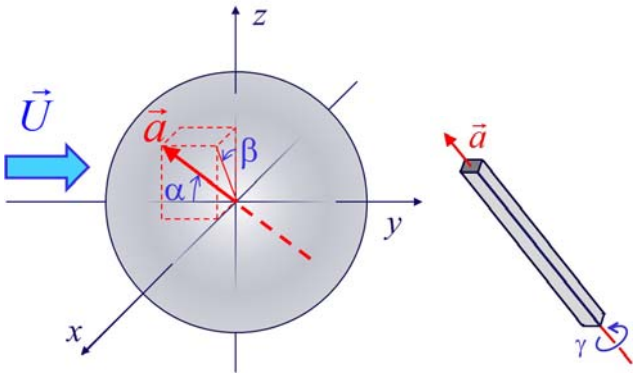

Figure 4. Definition of angles to express the orientation of main axis and yaw angle around it.

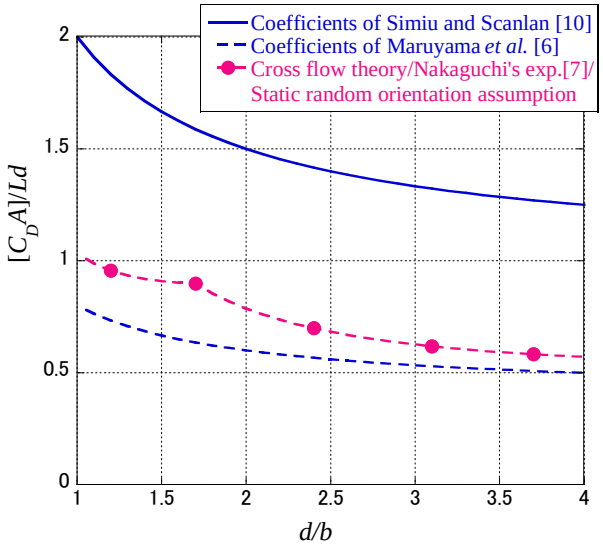

Figure 5. Effective drag coefficient, $[C_DA]/Ld$, in variation with the aspect ratio of the smallest rod cross-section, d/b.

Conclusions

The authors have examined the two kinds of flight parameter coefficients employed by Simiu and Scanlan [10] and Maruyama *et al.* [6] with particular focus on a rectangular rod. The numerical flight trajectories were obtained with the two kinds of flight parameter coefficients by numerically simulating rod motions in the wind tunnel experiment of Texas Tech University [3]. The comparison between the numerical flight trajectories and the experimental observations has indicated that the set of the flight parameter coefficients suggested by Simiu and Scanlan [10] is absolutely conservative, while that by Maruyama *et al.* [6] is practically conservative to represent the upper bound of the effective drag force during translational motion with tumbling. Since the aspect ratio of the Lin's experiment [3] was fixed at 1.98, effect of the aspect ratio on the effective drag coefficient was discussed using the cross-flow theory, Nakaguchi's experimental data [7] and the averaging technique for static drag force with random orientation [11, 12]. The insight developed through the discussion suggests that the conservative features of both the coefficient sets will be applicable to a rod with the other aspect ratios.

References

[1] Carassale, L., Freda, A., Brunenghi, M. M., Piccardo, G. & Solari, G., Experimental investigation on the aerodynamic behavior of square cylinders with rounded corners, *The Seventh International Colloquium on Bluff Body Aerodynamics and Applications* (*BBAA7*), Shanghai, China, 2012, 939-948.

[2] Laneville, A., Gartshore, I.S. & Parkinson, G.V., An Explanation of Some Effects of Turbulence on Bluff Bodies, *4th International Conference on Wind Effects on Buildings and Structures*, pp.333-341, London (Heathrow), United Kingdom, September 1975.

[3] Lin, N., Simulation of windborne debris trajectories, Master of Science thesis, Dept. of Civil Engineering, Texas Tech Univ., Lubbock, Texas, 2005.

[4] Lin, N., Holmes, J., & Letchford, C., Trajectories of Wind-Borne Debris in Horizontal Winds and Applications to Impact Testing, *Journal of Structural Engineering*, **133** (2), 2007, 274-282.

[5] Letchford, C., Lin, N. & Holmes, J., Wind-Borne Debris in Horizontal Winds and Applications to Impact Testing, in *Advanced Structural Wind Engineering*, editors Y. Tamura, A. Kareem, 2013, 197-215.

[6] Maruyama, T., Kawai, H., Okuda, Y. & Nakamura O., Numerical Study on Characteristics Debris in Tornado, *Annuals of Disaster Prevention Research Institute*, **57(B)**, 2014, 248-259. (in Japanese)

[7] Nakaguchi, H., Hashimoto K. & Muto, S., An Experimental Study on Aerodynamic Drag of Rectangular Cylinders, *The Journal of the Japan Society of Aeronautical Engineering*, **16** (168), 1968, 1-5. (in Japanese)

[8] Richards, P.J., Williams, N., Laing, B., McCarty, M. & Pond, M., Numerical Calculation of the Three-Dimensional Motion of Wind-borne Debris, *Journal of Wind Engineering and Industrial Aerodynamics*, **96**, 2008, 2188-2202.

[9] Richards, P.J., Steady Aerodynamics of Rod and Plate Type Debris, *17th Australasian Fluid Mechanics Conference*, 2010.

[10] Simiu, E. & Scanlan, R. H., *Wind effects on structures: fundamentals and applications to design*, 3rd Edition, John Wiley & Sons, Hoboken, NJ, 1996.

[11] Twisdale, L.A., Dunn, W.L. & Davis, T.L., Tornado Missile Transport Analysis, *Nuclear Engineering and Design*, **51**, 1979, 295-308.

[12] Twisdale, L.A. & Vickery, P.J., Comparison of Debris Trajectory Models for Explosive Safety Hazard Analysis, *25th DoD Explosive Safety Seminar*, Anaheim, California, 1992.